Published in final edited form as:
Anal Chem. 2009 September 1; 81(17): 7428–7435. doi:10.1021/ac901265t.

Nanocapillaries for Open Tubular Chromatographic Separations of Proteins in Femtoliter to Picoliter Samples

Xiayan Wang[†], **Chang Cheng**[†], **Shili Wang**[†], **Meiping Zhao**[‡], **Purnendu K. Dasgupta**[§], and **Shaorong Liu**[*,†]

[†]Department of Chemistry and Biochemistry, The University of Oklahoma, Norman, Oklahoma 73019, USA

[‡]College of Chemistry and Molecular Engineering, Peking University, Beijing 100871, P.R. China

[§]Department of Chemistry and Biochemistry, The University of Texas at Arlington, Arlington, Texas 76019, USA

Abstract

We have recently examined the potential of bare nanocapillaries for free solution DNA separations and demonstrated efficiencies exceeding 10^6 theoretical plates/m. In the present work, we demonstrate the use of bare and hydroxypropylcellulose (HPC) coated open tubular nanocapillaries for protein separations. Using 1.5 μm inner diameter (i.d.) capillary columns, hydrodynamically injecting femto to picoliter (fL-pL) volumes of fluorescent or fluorescent dye labeled protein samples, utilizing a pneumatically pressurized chamber containing 1.0 mM sodium tetraborate solution eluent (typ. 200 psi) as the pump and performing on-column detection using a simple laser-induced fluorescence detector, we demonstrate efficiencies of close to a million theoretical plates/m while generating single digit μL volumes of waste for a complete chromatographic run. We achieve baseline resolution for a protein mixture consisting of transferrin, α-lactalbumin, insulin, and α -2-macroglobulin.

Introduction

Since the pioneering work of Horvath and co-workers1,[2] in liquid chromatography (LC), there has been a continuous interest in performing LC separations in ever smaller scales. Various forms of capillary LC highlight this trend.[3-6] There are many benefits of downsizing LC columns: Low sample requirement, negligible waste generation, improved resolution, increased separation speed, ability to use exotic eluents, and so on.

There are also many hurdles: One needs injection valves capable of introducing pL-nL sample volumes, high pressure pumps capable of generating stable flows at nL-μL/min flow rates, pL-nL volume connectors capable of sustaining high pressures and detectors capable of detecting pL-nL volume eluite bands. This situation has improved in recent years. For example, injection valves with 10-20 nL injection volumes are now commercially available (see, e.g., www.vici.com), dispensing pumps based on microsyringes or a new generation of bidirectional precision pumps7 are commercially produced, pL-volume connectors have been microfabricated,8 and on-column laser-induced fluorescence (LIF) detectors can routinely detect fluorescent molecules just a few hundred in number.[9] Issues nevertheless remain for practical capillary LC. Open tubular liquid chromatography (OTLC)10-15 utilizes open

*Corresponding Author: †Department of Chemistry and Biochemistry, The University of Oklahoma, Norman, OK 73019 Email: shaorong.liu@ou.edu.

capillaries with inner diameters normally ranging from a few to tens of micrometers. In addition to the advantages common to all capillary LC formats, OTLC does not require high-pressure pumps. The theoretical limitations and characteristics of microcolumn chromatography were originally discussed in detail by Knox and Gilbert,16 and Knox.17 With larger diameter open tubular columns, the mass transfer between stationary and mobile phases becomes the rate limiting factor. Theoretically, this issue can be addressed by reducing the column diameter. The separation efficiencies (in terms of the number of theoretical plates per unit column length) are predicted to increase with decreasing column diameter; $>10^6$ plates/m are predicted to be possible with sub-micrometer diameter capillaries.

The quest to continually improve efficiency has been unending ever since liquid phase chromatography was invented.18 The advent of uniformly packed columns was a major breakthrough;19¯20 such columns provided fine and uniform pathways for the mobile phases to pass through. Each pathway can be considered equivalent to the bore of an open capillary tube. The smaller the diameter of these pathways, shorter is the mass transport time between the mobile and stationary phases. Accordingly, smaller and smaller particles are being used to improve the efficiency of packed LC columns.[21] The highest density packing possible with uniform spheres is hexagonal close packing (HCP). In HCP, both tetrahedral and octahedral voids are formed, and the largest spheres that can fit through these voids respectively have diameters of 0.225*d* and 0.414*d* where *d* is the diameter of the individual spheres.[22] The average pathway diameters for columns packed with the present state of the art 1-2 μm dia. nonporous spherical particles range between 400-800 nm;[23] this falls short of the above idealized goals. Nevertheless, the high efficiencies with these columns can be viewed as a direct consequence of the reduction of these pathway diameters.

We have recently utilized sub micrometer (nominally 500 nm as stated by the manufacturer, more recently measured by us by scanning electron microscopy to be 750 nm, see Figure S1 in supporting information, (SI)) radius open tubes, ~0.5 m long, to separate DNA molecules; with pneumatically driven eluents at ~100 psi, we routinely observed efficiencies $>10^6$ plates/m.[24] In the present manuscript, we observe that hydrodynamically injected fL-pL volumes of fluorescently labeled protein samples, containing a few hundred to a few thousand copies of protein molecules in the aliquot, can be separated with nearly as high efficiencies and detected in the same manner. We discuss both the potential possibilities and the paradoxes associated with this approach to protein analysis.

EXPERIMENTAL SECTION

Reagents and Materials

α-2-Macroglobulin (from human plasma, www.mpbio.com), Recombinant Aequorea coerulescens green fluorescent protein (rAcGFP1, www.clontech.com), human transferrin (www.lifetech.com) and ATTO-TAG™ FQ amine derivatization kit (www.invitrogen.com) were purchased as indicated. All other proteins, sodium dodecyl sulfate (SDS) and hydroxypropylcellulose (HPC) were from www.sial.com. Sodium hydroxide, methanol, and sodium tetraborate decahydrate ($Na_2B_4O_7$) were from www.fishersci.com; all fused-silica capillaries were from www.polymicro.com; nanocapillaries (360 μm o.d., 1.5 μm i.d.) were custom-made. All solutions were prepared using ultrapure water (UPW, Barnstead Nanopure, www.thermo.com) and filtered through a 0.22 μm filter (P/N 100370-922, www.vwrsp.com) and degassed by vacuum before use.

Apparatus

The experimental setup is schematically shown in Figure 1. The Helium-pressurized chamber, consisting of a cap and a base (7.8 mm i.d., 29.5 mm deep, accommodates a 600 μL

microcentrifuge tube to serve as a sample/eluent vial) was machined in-house from poly (methylmethacrylate). A septum was put between the base and the cap to ensure a seal. A high-pressure regulator was used to control the applied pressure (<500 psi). The line connecting the helium pressure line from the vent valve (Figure 1) to the solution chamber contains a stainless steel hypodermic needle tubing (25 ga. 3.5 cm long), this restriction protects against explosive helium release, even if the pressurized chamber fails. The sampling end of the nanocapillary was inserted through the septum into the solution vial. A detection window was made by removing a small section of the polyimide coating near the detection end of the nanocapillary. The nanocapillary detection window was held firmly in place with a house-designed capillary holder placed on an x-y-z translation stage (model M-460A-XYZ, www.newport.com). Detection was achieved with a confocal LIF detector, described previously.[25] Briefly, the output of a 488 nm laser (Spectra-Physics model 263, 25 mW, www.newport.com) was directed to a dichroic mirror (Q505LP, www.chroma.com) thus reflecting the beam to an objective lens (20×, 0.5 NA, www.rolyn.com) that focused it on the nanocapillary. The emitted fluorescence was collected and collimated by the same objective lens, passed through the dichroic mirror which removed most of the excitation light. The fluorescence emission was further filtered through a band-pass emission filter (centered at 535 nm, half bandpass 35 nm, www.omegafilters.com) and spatially filtered through an 0.8 mm diameter aperture onto a self-contained miniature photosensor module (H5784, Hamamatsu). The signal from the photosensor was acquired at 500 Hz by a 12-bit A/D converter (PMD-1208LS, www.mccdaq.com), and every 125 data points were averaged to create one signal output point. The data acquisition and processing were conducted using a LabVIEW™ (www.ni.com) program written in-house.

Fluorescence Labeling of Proteins

A 10 mM stock solution of ATTO-TAG™ FQ was prepared by dissolving 5.0 mg of the solid in 2.0 mL methanol. A 0.20 M KCN stock solution was prepared by dissolving 20 mg of KCN in 1.5 mL of UPW. Working KCN solution (10 mM) was prepared just before use. Protein solutions (each containing only one protein at 1 mg/mL) were prepared in 1% SDS and stored at -80 °C. To start the labeling reaction, a protein solution was denatured at 95 °C for 5 min. 5.0 μL of the denatured protein sample was mixed with 10 μL of the 10 mM KCN working solution and 10 μL of the 10 mM FQ solution in a vial, and this mixture was maintained at 65 °C for 5 min. The resulting FQ-labeled-protein was diluted with an appropriate buffer solution and stored on ice prior to analysis. Intrinsically fluorescent, the rAcGFP1 protein did not require FQ labeling.

Preparation of HPC-coated capillary

HPC was dissolved in UPW at a concentration of 1.0% (w/w). The nanocapillary was flushed for 1 h with the HPC solution under a pressure of 300 psi He. Afterwards, capillary was simply lifted up from the liquid to the headspace such that the HPC solution was blown out under the same gas pressure; however, a thin layer of HPC solution was left on the capillary interior wall. To immobilize the HPC on the surface, the capillary was put in an oven at 140 °C for 20 min while helium was simultaneously made to flow continuously through it. These steps (solution flushing, blowing out and immobilization) were repeated 5 times.

Nanocapillary Alignment for Detection

Because of the small bore dimensions, proper optical alignment was critical. A 10 μM fluorescein solution was allowed to flow continuously through the capillary at a constant pressure to avoid complications from photobleaching. The capillary position was adjusted by the micropositioners in all three dimensions until the maximum fluorescence signal was reached. All three positioners were then locked. The nanocapillary was flushed next with UPW

until the fluorescence signal decayed to the background level; the eluent was next flushed through it.

Sample Injection and Analysis

For sample injection, a vial containing a sample solution was placed inside the pressure chamber, and the chamber was capped and sealed. With the three-way valve set at vent (see Figure 1), the sampling end of the nanocapillary was inserted into the solution inside the vial. The three-way valve was then switched to a sample injection position (as shown in Figure 1) so that pressure-regulated helium gas was introduced into the pressure chamber, and the sample was pressurized into the nanocapillary. After a preset period of time, sample injection was stopped by switching it back to vent. A timer was used to control the sample injection duration. As an example, based on the Poiseuille equation,[26] for a 1.5 μm i.d. 47 cm long column, the computed injection volume is 1.86 fL/(psi.s), or in term of injected sample length, 1.06 μm/(psi.s). After the sample injection, the sampling end of the nanocapillary was transferred to another pressure chamber in which a vial containing the eluent was placed, and a desired pressure (typ. 100-300 psi) was applied to the chamber to carry out the separation.

Measurement of Void Times

A fluorescent dye [methyl 2-(3-(2-iodoethoxy)-6- oxo-6*H*-xanthen-9-yl)benzoate (MIOXB, structure shown in scheme S1 in SI) was used for these measurements. This dye is neutral over a wide pH range (pH=2-11) and shows no significant to adsorb on silica surfaces. To measure the void time, the dye was dissolved in methanol, injected into the capillary column with the borax solution flowing through it at the pneumatic pressure of interest and detected with the above LIF detector. The elution time was considered to be the void time.

RESULTS AND DISCUSSION

Mechanistic Aspects of Separations in Nanocapillaries

In the pressure-driven bare nanocapillary format, we have previously separated diverse samples ranging from ssDNA and dsDNA fragments (a few to tens of thousands of base pairs)[24] to small anionic or fluorescent dyes.27 One of the outstanding aspects of these separations has consistently been the paradoxical situation that the analytes elute *before* the void times of the column. Note that void times were assessed both from (a) the internal volume ($\pi r^2 L$) and the flow rate F as computed from the Poiseuille equation ($F = (\Delta P \pi r^4)/(8\eta L)$, see SI) and (b) from the retention time of MIOXB, an unretained dye. The two sets of data agreed well, confirming both the accuracy of the geometrical dimensions, the applicability of the Haagen-Poiseuille equation and lack of adsorption of the MIOXB probe on the capillary walls. We also conducted some experiments with a conventional HPLC pump and a splitter capillary; virtually the same results were obtained at the same flow rates. However, the use of the splitter requires use of much larger amounts of the purified protein samples and this was not further pursued.

Elution of analytes before the void time (as measured with a small unadsorbed probe molecule) is common in a number of chromatographic modes, these include hydrodynamic chromatography,28 size exclusion chromatography29 and ion exclusion chromatography.30 In previous work involving the separation of DNA molecules in a naocapillary25 we surmised that elution before the void time occurs because the negatively charge analytes are excluded from the regions near the negatively charged walls and stay closer to the center, thus experiencing a mean axial velocity greater than the mean velocity that includes zero velocity at the boundary layer and that corresponds to the void time. Accordingly, the quadruply negatively charged bis(2-carboxyethyl)- carboxyfluorescein was observed to elute before the fluorescein monoanions, that in turn eluted before neutral Rhodamine B; a theoretical model could account for this behavior.[25] It was shown that if the capillary was coated with HPC to

render the wall zeta potential essentially to zero, the above dyes could no longer be separated. In the present case, HPC coating does not alter the retention or the separation so a charge based exclusion cannot be the basis of separation in the present case.

We believe instead that the basis of separation in the present case lies elsewhere. There is an aspect of conducting chromatography of very large molecules in very small diameter columns that has not been discussed. Whereas a small molecule analyte is infinitesimally small relative to the bore of the column and can indeed truly experience being at the boundary wall, this is not the case when we consider a very large molecule in a very small diameter column. At the minimum, the effective column diameter in this case is the difference of the actual diameter and the hydrodynamic diameter of the molecule because that is the maximum extent of translation in the radial direction that the analyte can undergo. The Stokes diameter of GFP is ~5 nm (see SI). Minimally, while one end of the molecule is at the boundary wall, the other end will experience a velocity that corresponds to the axial velocity that is characteristic of the axial velocity 5 nm from the wall. If the molecule assumes a more elongated conformation in the flow-field than static solution or if the conformation of the molecule itself is dependent on the precise flow field it is experiencing (meaning that the conformation changes dynamically depending on radial position), this can provide a basis for separation. Admittedly, this is a hypothesis: much still needs to be done before the separation mechanism is fully elucidated.

Chromatographic Behavior of Green Fluorescent Protein in the Pressure Driven Nanocapillary System

We use this to illustrate typical behavior of a largely unretained protein[31]. Figure 2 is a chromatogram for the elution of rAcGFP1. The main panel shows the raw data that were acquired at 4 Hz. The inset (a) shows an abscissa-magnified view of the elution profile and a gaussian fit to the eluite peak while the inset (b) shows the same data except after processing through a 20-point moving average filter (*n*-point averaging was attempted for many values of *n*; *n*=20 is a compromise between improved S/N and decreasing column efficiency) that improves the S/N by ~3.5x, although some of loss of efficiency and peak height does occur. As observed in Figure 2, t_R for rAcGFP1 is 21.3 min, the computed void time is 23.2 min (see SI). Because of uncertainties in temperature and capillary bore and the uniformity of the same, these values are not really distinguishable from each other. In fact, the retention behavior of rAcGFP1 was also investigated on an identical HPC-coated column; it produced results that were very similar to that for the bare capillary, suggesting that in this case charge on the capillary wall has little or no effect. This is true even though acGFP1 has a PI of 5.57-5.99[32] and must be negatively charged in a medium containing 1 mM $Na_2B_4O_7$.

The concept of the height equivalent of a theoretical plate (H) applies, whether or not there is retention on the wall or any interactions with the wall. We define H in the usual manner as the column length L divided by the number of theoretical plates N:

$$H=L/N \tag{1}$$

where N of a Gaussian peak of half width $W_{0.5}$ eluting at time t_R is given by:

$$N=5.54(t_R/W_{0.5})^2 \tag{2}$$

There are many studies that relate to the relevant aspect of calculating the diffusion coefficient of a solute by measuring the half-width of the band moving at a velocity *u* cm/s through a tube,[33-36] based on the original work of Taylor,[37-39] as modified by Aris.[40] Golay[41] derived, for an open tube with no stationary phase:

$$H = \frac{2D_m}{u} + \frac{u \cdot d^2}{96 D_m} \quad (3)$$

The diffusion coefficient (D) of GFP has been measured to be is 8.7×10^{-7} cm^2/s.[42] Using diameter $d = 1.5 \times 10^{-5}$ cm and using the observed value of u (3.44×10^{-2} cm/s; 44 cm in 21.3 min) as observed, we obtain H = 0.57 μm. It is noteworthy that 83% of this plate height contribution comes from the first term that can be considered to be the irreducible, time-dependent intrinsic diffusive contribution. The above corresponds to a theoretical maximum efficiency of 1.75×10^6 plates/m, and because of the dominance of the first term in eqn. 3, it has relatively little dependence on the capillary diameter. In comparison, Figure 2a has a peak half-width of 4.84s (0.167 cm), from which we compute $N = 3.86 \times 10^5$ (8.8×10^5 plates/m) from eqn. 2 and H = 1.14 μm from eqn. 1. It is remarkable that the efficiency we observe is 50% of the ideal theoretical behavior.

In fact, much of the shortfall from theory can be accounted for. The injection pressure and duration (100 psi, 10 s) in Figure 2 results in a 1.86 pL injected plug that is 1.06 mm long in the capillary (this ignores any broadening during in the injection process), this sample zone length is far from negligible compared to the observed peak half-width of 1.67 mm; idealized behavior can only be obtained with a sample plug that is infinitesimally narrow. Nevertheless, considering that band broadening adds in a root mean square fashion, we can estimate that had the injection been infinitesimally small (in practice, of course, detection will not be possible in a real case), the observed half bandwidth would have been 1.29 mm $\left(\sqrt{\left(1.67^2 - 1.06^2\right)}\right)$ equivalent to 3.75 s, leading to $N = 6.43 \times 10^5$ plates (1.46×10^6 plates/m) and H = 0.68 μm. This now corresponds to 83% of the theoretical maximum. A second important factor that we believe also contributes to some loss of efficiency is inadequate data acquisition rate. However, a faster data acquisition rate may not be very practical with the present equipment; the averaging carried out to go from Figure 2a to 2b results in nearly 2× loss of plate counts. All other data shown in this paper utilizes results based on the 20-point averaging procedure. The rAcGFP1 solution injected was 5.0 ng/μL (~0.18 μM) in concentration. Under the experimental conditions, ~200,000 molecules were injected. Referring to trace B, the rAcGFP1 peak has an S/N = 50, demonstrating an S/N = 3 limit of detection <12,000 molecules. This LOD was obtained with a rather simple detection system, and an inexpensive photosensor module. It can doubtless be further improved with an optimized system that utilizes a higher magnification objective with a greater numerical aperture, a sheath-flow cell[43] and a photon-counting detector. For a cell with a diameter of 10-20 μm (typical for most human cells), the fluid volume is in the low pL range. Even with the present detection system, this approach is likely to have sufficient sensitivity to carry out the determination of at least the major protein components, appropriately tagged, in single cells.

Separation of Protein Mixtures - Effect of Eluent Composition

Through the rest of this manuscript we characterize the separation behavior of the system using a protein mixture where the analytes elute in this order: (a) transferrin (MW - 76 kD, p*I* = 5.9), (b) α-lactalbumin (MW - 14.2 kD, p*I* = 4.8), (c) insulin (MW - 5.7 kD, p*I* = 5.5), and (d) α-2-macroglobulin (MW - 170 kD, p*I* =5.4). Obviously this elution order cannot be predicted by any simple consideration of size or charge; rather, we believe that this elution order is a result of the different topologies of these protein molecules, and the ability of certain regions of the macromolecule to access the capillary wall and the quantitatively varying interactions of these with the wall.

Figure 3 shows the chromatogram of the four proteins at various different $Na_2B_4O_7$ eluent concentrations. It will be noted that the chromatographic behavior is greatly affected by the eluent composition. One makes the curious observation that chromatographic efficiencies improve but selectivity decreases as the eluent concentration is increased. Except for α-2-macroglobulin, the retentions of all the other proteins increase with increasing eluent concentration. For α-2-macroglobulin (the last peak) retention decreases with increasing [$Na_2B_4O_7$] from 0.1-1.0 mM but increases thereafter. In Figure 4, we plot log t_R vs. log [borate anion], the latter computed based on the pK_a of the acid.[44] It is apparent from Figure 4 that the slope of the line between the lowest two (or three) eluent concentrations for each plot is different from those for the respective plots at higher concentrations. The lower concentration slopes start with a positive value for transferrin and decrease in magnitude, becoming ~zero for insulin and for α-2-macroglobulin, this is actually negative at the beginning. However, the slopes at the higher concentrations are different for the different proteins, decreasing in the order transferrin> α-lactalbumin> insulin> α-2-macroglobulin. These differing slopes result in the retention values that approach each other at high concentrations and as a result, despite improved efficiencies, selectivity and hence resolution, is lost. This was presumably due to the protein conformation changes with the concentrations. The conformations of these proteins likely differ to a greater extent at low concentrations while at high ionic strengths they all assume the most tightly packed conformation where the exterior exposed surface area is minimized

Similar results, notably that resolutions deteriorate while separation efficiencies improve with increasing eluent concentration, were also observed with NaOH as eluent (detailed data are shown in Figure S3 in SI). SDS was also tested as an additive in the eluents, but there was no beneficial effect on the separation (Figure 5). The concentrations used here are below the critical micelle concentration of SDS. Any adsorption of the surfactant, either on the wall (unlikely, as the wall is already negatively charged) or association with the analyte (unlikely, because above the pI, the analyte is also negatively charged), is expected to reduce the retention. Paradoxically, as the log t_R -log [SDS] plot in the inset indicates, the retention increases on SDS addition. The log t_R - log[SDS] plots are almost linear with positive slopes but the slopes differ among the analytes in a manner that much like increasing eluent concentration, addition of SDS results in loss of selectivity. Further work was carried out solely with 1.0 mM $Na_2B_4O_7$ as eluent, without additives.

Effect of Capillary Inner Diameter

Capillary diameter is a key parameter that affects the separation efficiency. We have tested capillaries with three different diameters (1.5 μm, 2.4 μm, and 4.2 μm). Figure 6 presents the separation results when all other experimental conditions were maintained the same (including column lengths: 50 cm total and 45 cm effective and eluent pressure 150 psi). With the 4.2-μm capillary, the analytes eluted fast and without resolution. With the 2.4-μm capillary, the analytes are nearly resolved; predictably, even better resolution is obtained with the even smaller 1.5 μm capillary. It is reasonable to conclude that efficiency and resolution will continue to improve with narrower capillaries. Presently extruded capillaries are not available in diameters that are still smaller but we hope to report on results of similar separations using nanofabricated channels in the near future.

Meanwhile it is interesting to note that based on the diameters and the applied pressure, the void retention times are 9.65, 29.5 and 75.7 min., respectively for the 4.2, 2.4 and 1.5 μm i.d. capillaries; all of the traditionally computed k' from the largest to the smallest capillary are negative. Table S1 in SI lists the values; these do not scale with capillary bore in any consistent manner.

The results of a different experiment, where at a constant applied pressure the length of the larger capillaries were adjusted until almost the same retention time was obtained for the group of analytes is shown in Figure 7. Detailed numerical data are shown in Table S2 in SI for the two smaller bore capillaries, it is interesting that although the resolution is better for the smallest bore capillary, the efficiency in terms of the number of plates (for all but transferrin, also plates/m) is the best for the intermediate bore capillary.

The Effect of Flow Rate (Elution Pressure)

The effect of elution rate (or elution pressure) on both resolution and separation efficiency was systematically examined for a 70 cm long 1.5 μm i.d. capillary. We measured the resolution between the transferrin and the lactalbumin peaks as well as the respective plate heights. As shown in Figure 8, both the optimum resolution and efficiency was obtained at a pressure of ~200 psi; low μm plate heights were routinely obtained. We expect that the optimum pressure will change with the proteins selected and other experimental parameters such as eluent composition and capillary dimensions. An elution pressure higher than that optimum for maximum efficiency may often be desirable to increase separation speed.

Effect of Column Length

The effect of capillary length on separation performance was tested using 1.5 μm i.d. capillaries 50-110 cm in length using a constant pressure gradient; the results are shown in Figure 9. As with conventional columns, the resolution values between the analytes increase with increasing capillary length. For hard to resolve molecules, increasing the column length, as practiced in conventional separations, will also apparently be a straightforward solution. However, this is carried out at the expense of reduced separation speed. Table S3 in SI shows detailed performance data for the different column lengths. It will be noted that which specific column generates the maximum plate counts, plates/m or plates per unit time varies from one analyte to another.

Capillary Surface Coating

Surface charge has been considered to have great impact on separations of charged molecules.[22,25,45,46] When we coated the nanocapillary with HPC (essentially eliminating the zeta potential) and used it for the same separations, no significant difference could be observed albeit the HPC-coated capillary may have provided a marginally more efficient separation (see Figure S4 and Table S4 in SI). This implies that electrostatic interaction is not the prevailing mechanism for the retention of the proteins or their separations. However, this does not preclude surface charge on the capillary walls affecting the conformation of a protein analyte molecule. The precise conformations of the protein molecules in a capillary of radial dimensions comparable to that of the analytes themselves has never been elucidated, the detailed separation mechanism is not fully understood. It is possible that hydrodynamic separation[28] and radial migration[47] both play significant roles in the separations. We continue to try to unveil the mechanism for separation of biomolecules in nanocapillaries, and hope to communicate the findings in the near future.

We have demonstrated protein separations in open tubular nanocapillaries, with high chromatographic efficiencies. With a very simple LIF detector, we can attain limits of detection of a few thousand molecules. With single molecule detection strategies that are presently common[48,49] and seemingly straightforward to adapt to the present nanocapillary, the detection limits can be vastly improved. Using pressure/hydrodynamic injection, we need only femtoliters to picoliters of sample for each separation. Most cells can provide this volume of sample; this separation technique, combined with micro/nanofluidic manipulations,[50,51] can thus be a powerful tool for single cell analysis.

Supplementary Material

Refer to Web version on PubMed Central for supplementary material.

Acknowledgments

This work is partially supported by NIH (1R21EB008512-01A1), NSF (CHE-0514706), and OCAST (AR082-051).

LITERATURE CITED

(1). Horvath CG, Preiss BA, Lipsky SR. Anal. Chem 1967;39:1422–1428. [PubMed: 6073805]
(2). Horvath CG, Lipsky SR. Anal. Chem 1969;41:1227–1234. [PubMed: 5797315]
(3). Ishii D. Jasco Report 1974;11:1–7.
(4). Hibi K, Ishii D, Fujishima I, Takeuchi T, Nakanishi T. J. High Resolut. Chromatogr. Chromatogr. Commun 1978;1:21–27.
(5). Tsuda T, Novtny MV. Anal. Chem 1978;50:623–634.
(6). Dandeneau RD, Zerenner EH. J. High Resolut. Chromatogr. Chromatogr. Commun 1979;2:351–356.
(7). Global FIA Inc.. Milligat Pump. http://www.globalfia.com/ItemSheets/MG.html (accessed June 2009)
(8). Liu S. Electrophoresis 2003;24:3755–3761. [PubMed: 14613202]
(9). Turner EH, Lauterbach K, Pugsley HR, Palmer VR, Dovichi N. J. Anal. Chem 2007;79:778–781.
(10). Ishii D, Tsuda T, Takeuchi T. J. Chromatogr 1979;185:73–78.
(11). Tsuda T, Tsuboi K, Nakagawa G. J. Chromatogr 1981;214:283–290.
(12). Tsuda T, Nakagawa G. J. Chromatogr 1983;268:369–374.
(13). Ishii D, Takeuchi TJ. Chromatogr. Sci 1984;22:400–410.
(14). Jorgenson JW, Guthrie EJ. J. Chromatogr 1983;255:335–348.
(15). Knecht LA, Guthrie EJ, Jorgenson JW. Anal. Chem 1984;56:479–482.
(16). Knox JH, Gilbert MT. J. Chromatogr 1979;186:405–418.
(17). Knox JH. J. Chromatogr. Sci 1980;18:453–461.
(18). Tswett MS. Ber. Deutsch. Bot. Ges 1906;234:384–393.
(19). Huber JFK. J. Chromatogr 1969;7:86–97.
(20). Kirkland JJ. J. Chromatogr. Sci 1969;7:7–12.
(21). MacNair JE, Patel KD, Jorgenson JW. Anal. Chem 1999;71:700–708. [PubMed: 9989386]
(22). Azaroff, LV. Introduction to solids. McGraw-Hill; 1960.
(23). Unger KK, Skudas R, Schulte MM. J. Chromatogr. A 2008;1184:393–415. [PubMed: 18177658]
(24). Wang X, Wang S, Veerappan V, Byun C, Nguyen H, Gendhar B, Allen RD, Liu S. Anal. Chem 2008;80:5583–5589. [PubMed: 18500828]
(25). Lu JJ, Liu S. Electrophoresis 2006;19:3764–3771. [PubMed: 16960840]
(26). Dasgupta PK. J. Liq. Chromatogr 1984;7:2367–2382.
(27). Wang X, Kang J, Wang S, Lu JJ, Liu S. J. Chromatogr. A 2008;1200:108–113. [PubMed: 18550070]
(28). Small H, Langhorst MA. Anal. Chem 1982;54:892A–898A.
(29). Hausler DW, Taylor LT. Anal. Chem 1981;53:1227–1231.
(30). Kunin R, McGarvey FX. Aanl. Chem 1962;34:48R–50R.
(31). Sun X, Yang W, Pan T, Woolley AT. Anal. Chem 2008;80:5126–5130. [PubMed: 18479142]
(32). http://www.clontech.com/products/detail.asp?tabno=2&catalog_id=632502&page=all&faq_id=154554
(33). Min Z, Li H-Y, Li Q, Yi C. Chin. Sci. Bull 2007;52:3325–3332.
(34). Sharma U, Gleason NJ, Carbeck JD. Anal. Chem 2005;77:806–813. [PubMed: 15679347]
(35). Yonezawa T, Tominaga T, Toshima N. Langmuir 1995;11:4601–4604.
(36). Grushka E, Kikta EJ Jr. J. Phys. Chem 1974;78:2297–2301.

(37). Taylor G. Proc. Roy. Soc. A London 1953;219:186–203.
(38). Taylor G. Proc. Roy. Soc. A London 1954;223:446–468.
(39). Taylor G. Proc. Roy. Soc. A London 1954;225:473–477.
(40). Aris R. Proc. Roy. Soc. A London 1956;235:67–77.
(41). Golay, MJE.; Desty, DH. Gas Chromatography. Academic Press; New York: 1956. p. 36
(42). Swaminathan R, Hoang CP, Verkman AS. Biophys. J 1997;72:1900–1907. [PubMed: 9083693]
(43). Crabtree HJ, Bay SJ, Lewis DF, Coulson LD, Fitzpatrick G, Harrison DJ, Delinger SL, Zhang JZ, Dovichi NJ. Electrophoresis 2000;21:1329–1335. [PubMed: 10826677]
(44). Dasgupta PK, Nara O. Anal. Chem 1990;62:1117–1122.
(45). Pennathur S, Santiago JG. Anal. Chem 2005;77:6772–6781. [PubMed: 16255573]
(46). Pennathur S, Santiago JG. Anal. Chem 2005;77:6782–6789. [PubMed: 16255574]
(47). Zheng J, Yeung ES. Anal. Chem 2002;74:4536–4547. [PubMed: 12236367]
(48). Lee J-Y, Li J, Yeung ES. Anal. Chem 2007;79:8083–8089. [PubMed: 17914754]
(49). Widengren J, Kudryavtsev V, Antonik A, Berger S, Gerken M, Seidel CAM. Anal. Chem 2006;78:2039–2050. [PubMed: 16536444]
(50). Huang B, Wu H, Bhaya D, Grossman A, Granier S, Kobilka BK, Zare RN. Science 2007;315:81–84. [PubMed: 17204646]
(51). Byun CK, Wang X, Pu Q, Liu S. Anal. Chem 2007;79:3862–3866. [PubMed: 17428033]

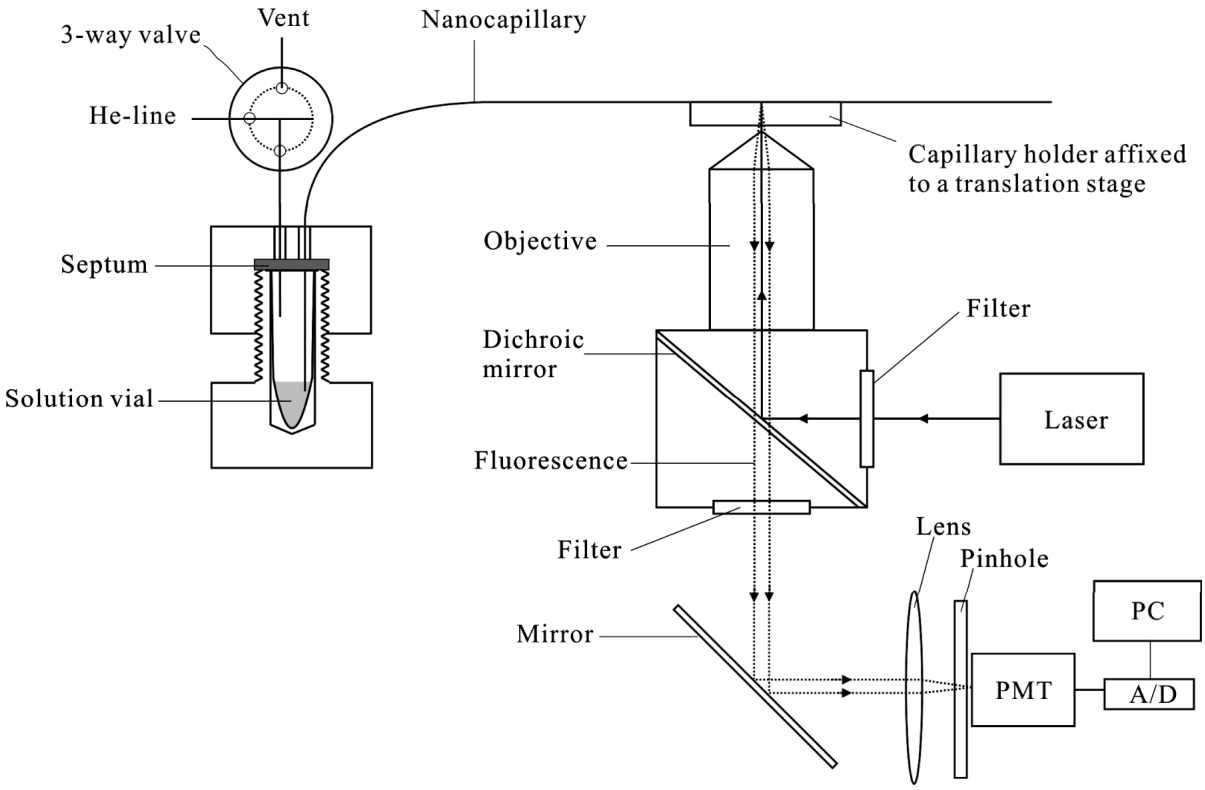

Figure 1.
Schematic diagram of the experimental setup

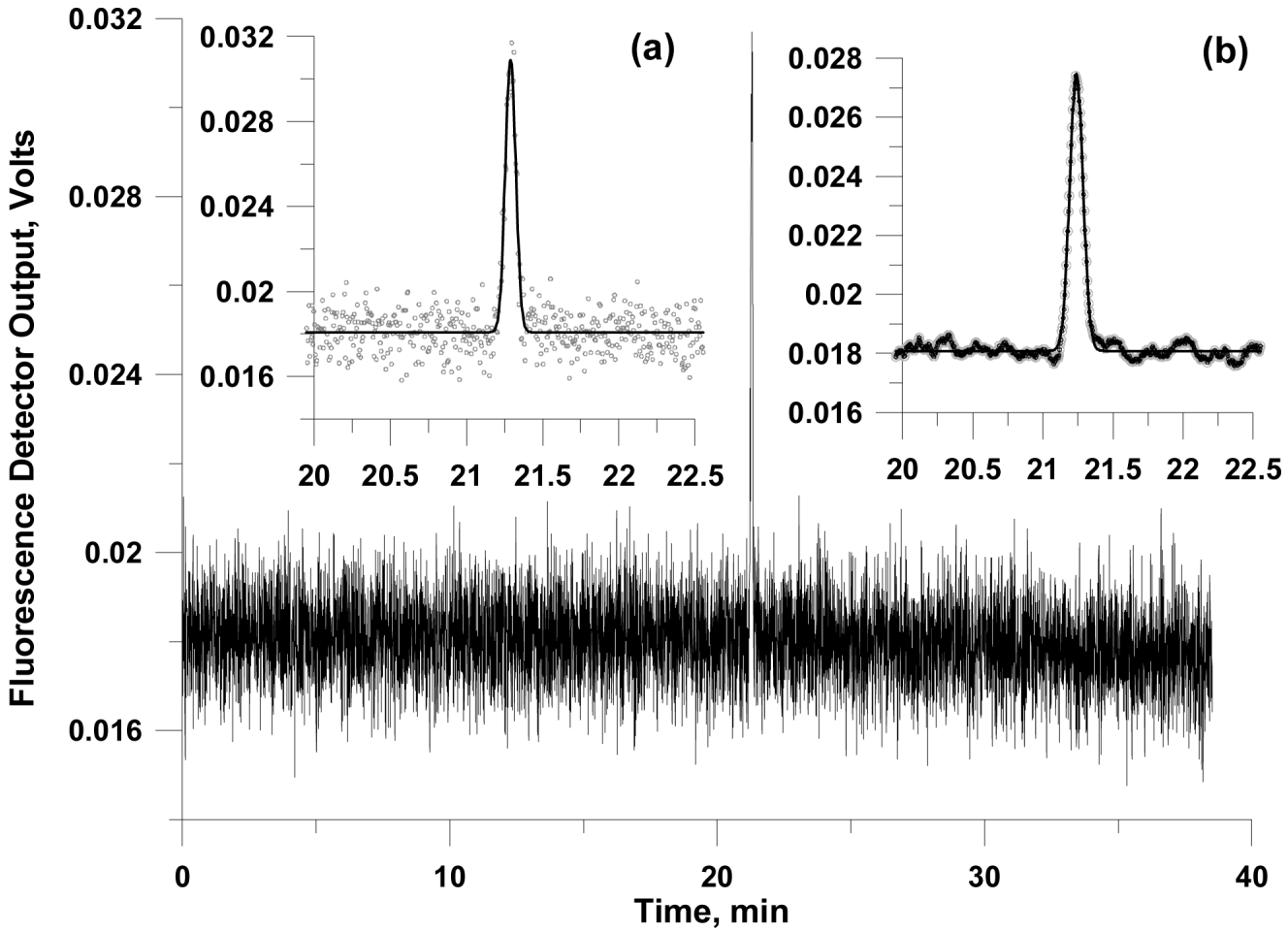

Figure 2.

Chromatogram showing the elution of rAcGFP1. The sample (5.0 ng/μL) was injected for 10 s@100psi. The column was 47 cm long (44 cm effective) and 1.5 μm in diameter. The eluent was 1.0 mM $Na_2B_4O_7$ pressurized at 300 psi. The principal trace is the raw data from the LIF detector. Inset (a) shows a gaussian fit to the eluite peak. Inset (b) shows the same data after a 20-point moving average filter.

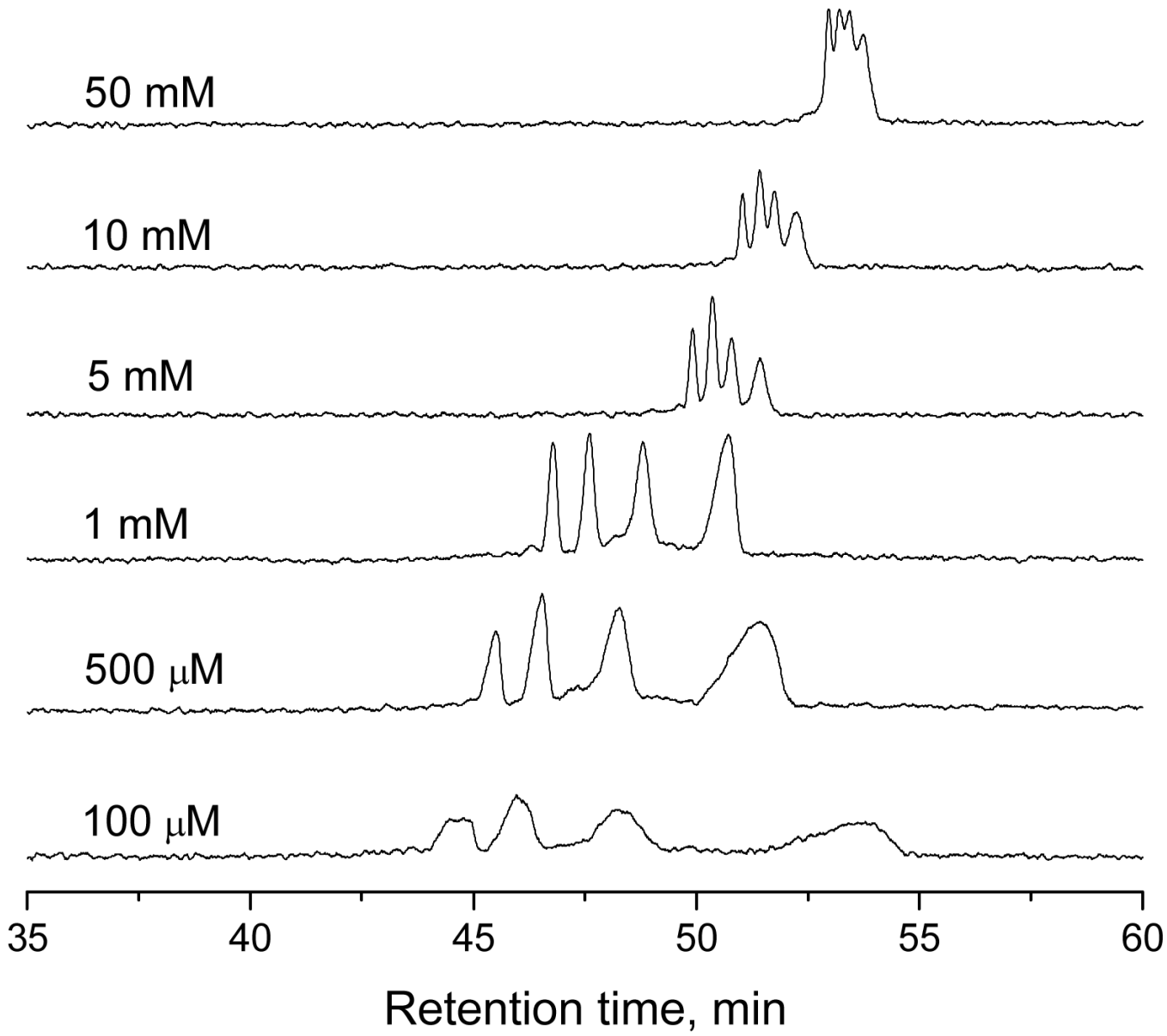

Figure 3.

Protein separation and the effect of sodium tetraborate concentration. The elution order remains the same, from left to right (1) transferrin, (2) lactalbumin, (3) insulin, and (4) α-2-macroglobulin. Capillary i.d. 1.5 μm, 70 cm long (65 cm eff.) Eluent pressure 300 psi. The analyte concentrations are 0.6 μM, 6.0 μM, 39.5 μM, and 0.03 μM, respectively. Samples were injected for 8 s@100 psi.

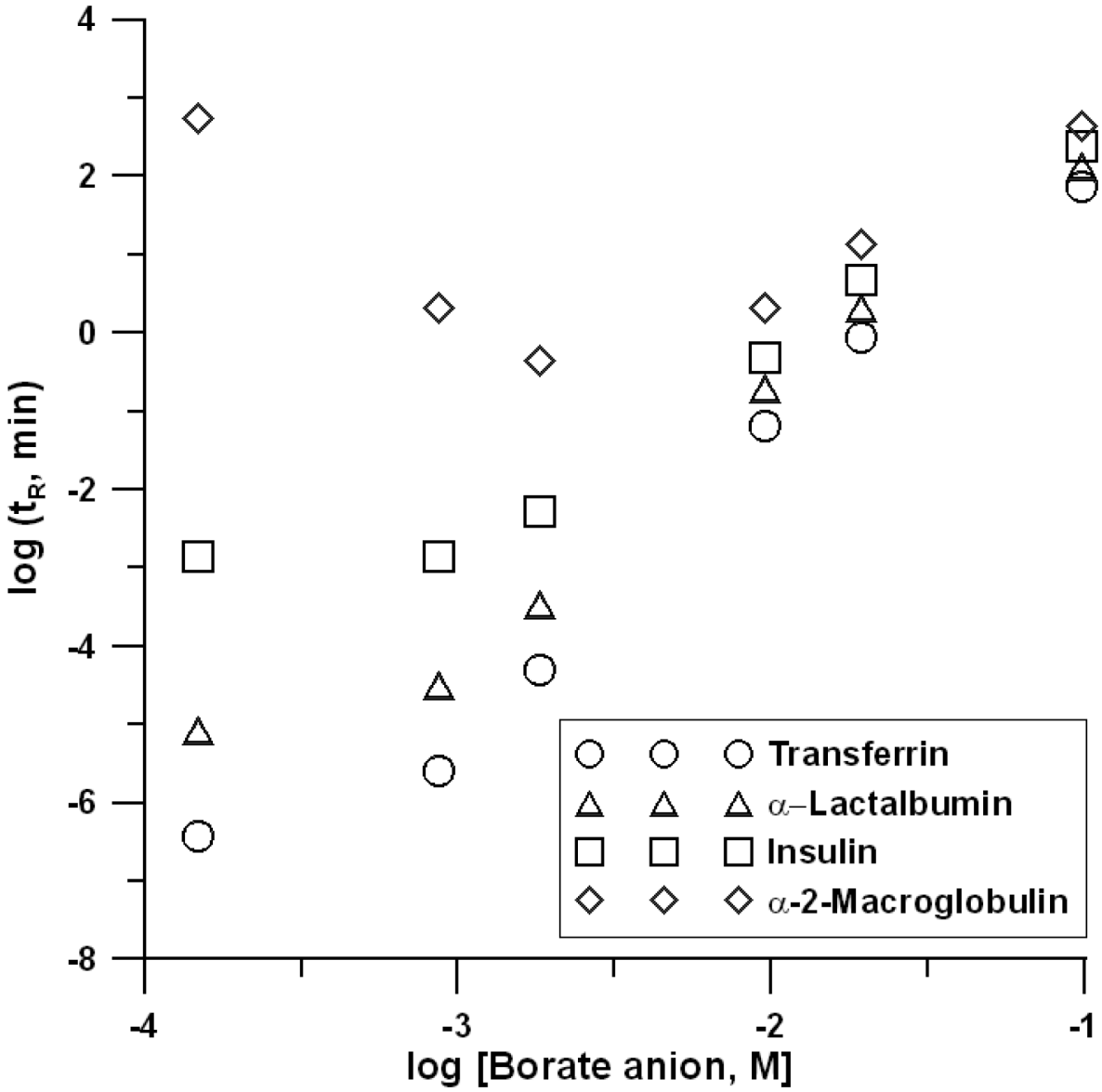

Figure 4.
Plot of log retention time vs. log eluent ion concentration. The slope changes are obvious in all cases above a borate anion concentration >1 mM, but is most notable for α-2-macroglobulin.

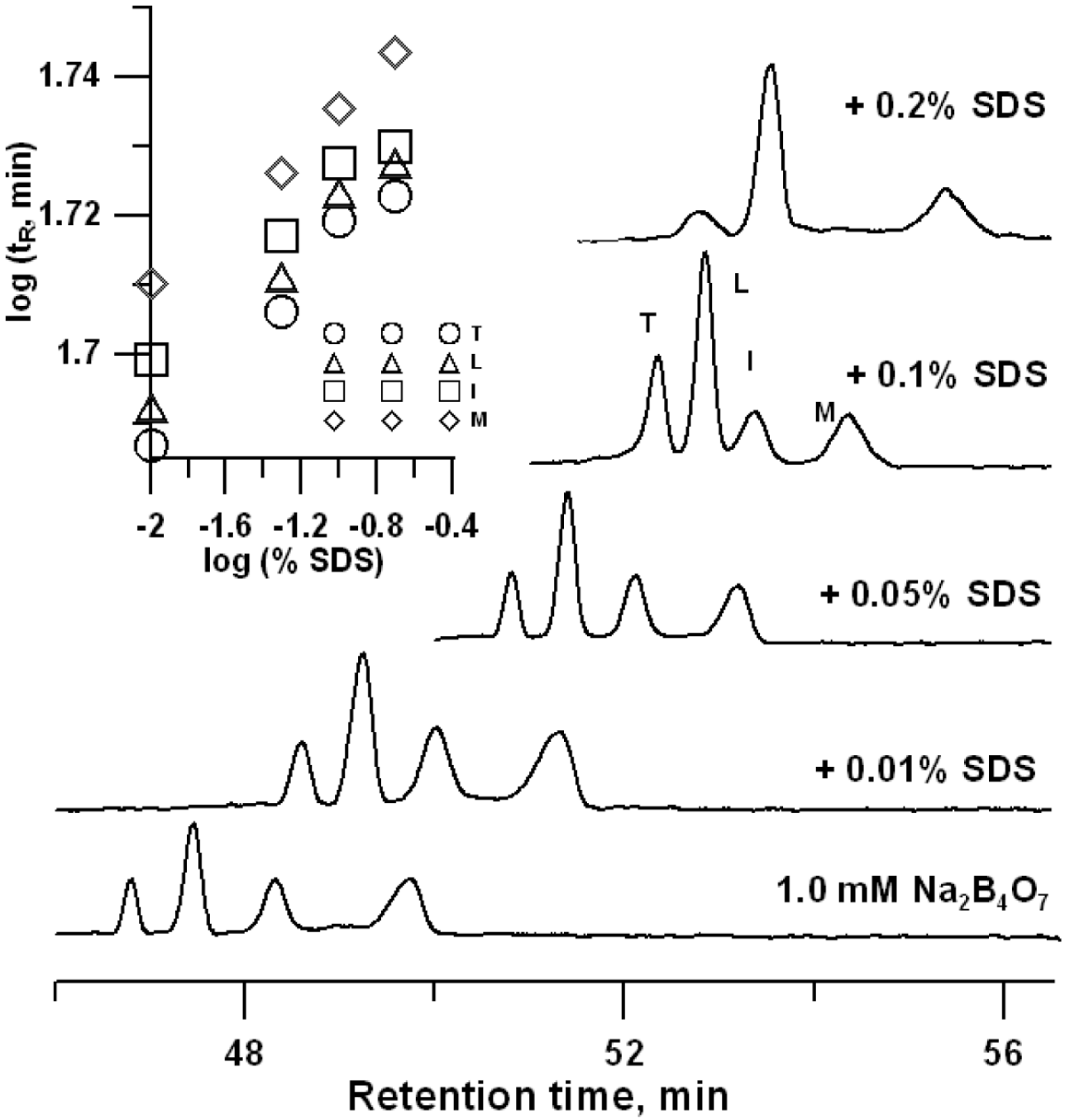

Figure 5.

Effect of SDS as an additive on the separation of the four proteins Transferrin (T), α-Lactalbumin (L), Insulin (I), and α-2-Macroglobulin (M) in a 1.5 μm i.d. 70 cm long (65 cm eff.) capillary at 300 psi. Samples were injected for 8 s@100 psi. The inset shows log t_R-log [SDS] plots.

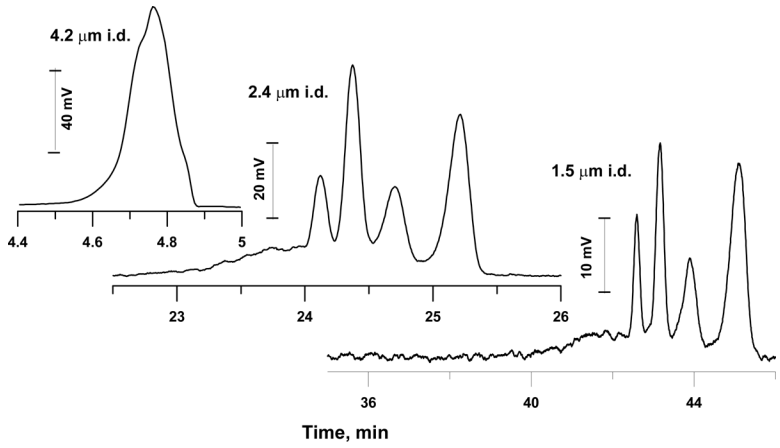

Figure 6.

All separation capillaries had the same length (50 cm total and 45 cm eff.). Sample injection duration and pressure were adjusted to ensure injections of sample plugs of nearly equivalent length with 4 s@15 psi for 4.2 μm capillary, 5 s@40 psi for 2.4 μm capillary and 8 s@100 psi for 1.5 μm capillary. Elution pressure 150 psi.

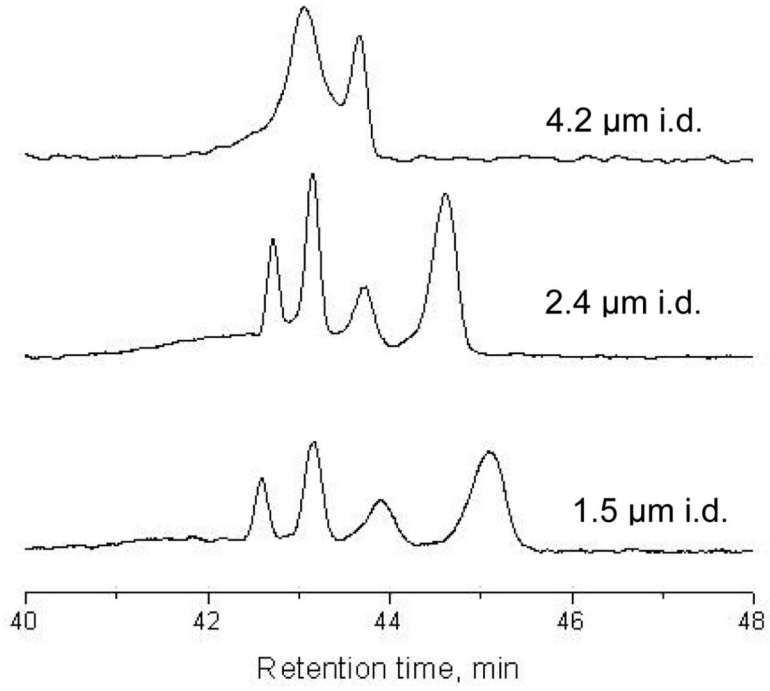

Figure 7.

The chromatograms were respectively obtained with a 155-cm long (150 cm eff.) x 4.2 μm i.d., a 70-cm long (65 cm eff.) x 2.4 μm i.d., and a 50-cm long (45 cm eff.) × 1.5 μm i.d. capillary. All sample injections were 8 s@100 psi and all separations were performed at 150 psi with 1.0 mM $Na_2B_4O_7$.

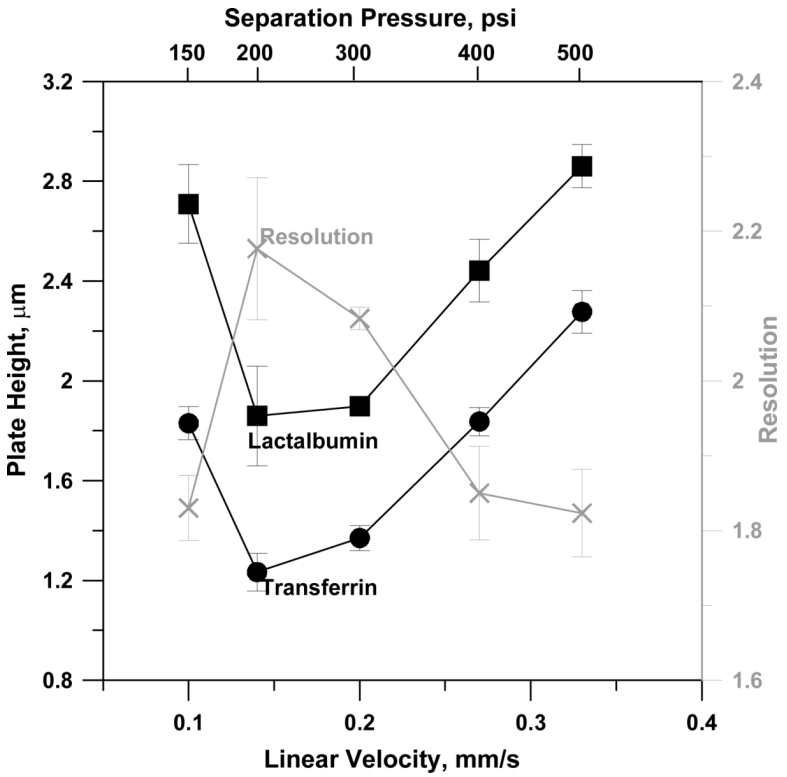

Figure 8.

Resolution between transferrin and α-lactalbumin as a function of linear velocity (separation pressure) on a 70 cm long (65 cm effective) × 1.5 μm i.d. capillary. Sample injections 8 s@100 psi; 1.0 mM $Na_2B_4O_7$ eluent.

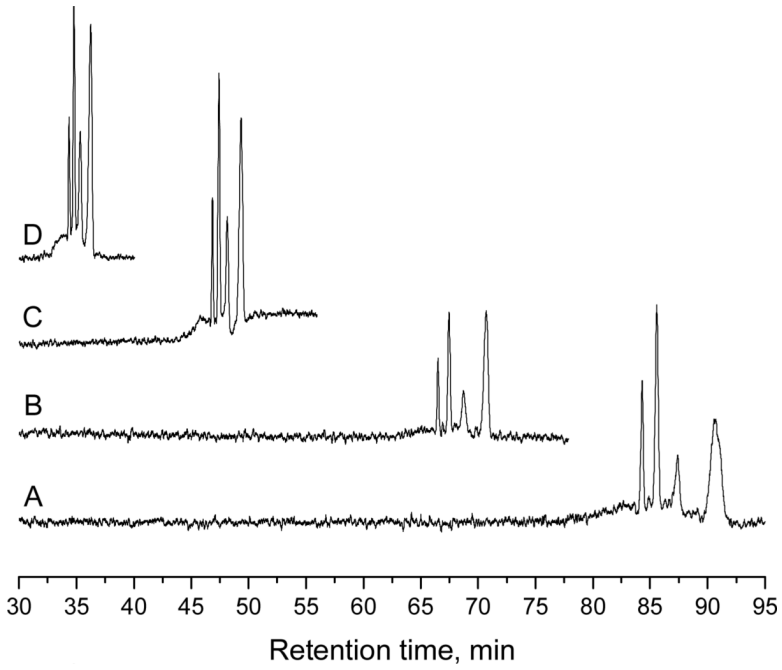

Figure 9.

Resolution as a function of capillary length. All separations were carried out under a constant pressure gradient (4.3 psi/cm column length) using 1.5 μm i.d. capillaries of (A) 110, (B) 90, (C) 70, (D) 50 cm lengths, the effective lengths in each case was 5 cm smaller. The eluent was 1.0 mM $Na_2B_4O_7$.